Changes in the molecular nodes of the Notch and NRF2 pathways in cervical cancer tissues from the precursor stages to invasive carcinoma

JARED E. LIMONES-GONZALEZ[1], PERLA AGUILAR ESQUIVEL[2], KARLA VAZQUEZ-SANTILLAN[3], ROSARIO CASTRO-OROPEZA[4], FLORIA LIZARRAGA[5], VILMA MALDONADO[5], JORGE MELENDEZ-ZAJGLA[6], PATRICIA PIÑA-SANCHEZ[4] and GRETEL MENDOZA-ALMANZA[5]

[1]Biotechnology Laboratory, Autonomous University of Zacatecas, Zacatecas 98160, Mexico; [2]Department of Pathology, Zacatecas General Hospital Luz González Cosío, Zacatecas 98160, Mexico; [3]Innovation in Precision Medicine Laboratory, National Institute of Genomic Medicine, Mexico City 14610, Mexico; [4]Molecular Oncology Laboratory, , Oncology Research Unit, XXI Century National Medical Center, IMSS, Mexico City 06720, Mexico; [5]Epigenetics Laboratory, National Institute of Genomic Medicine, Mexico City 14610, Mexico; [6]Functional Cancer Genomics Laboratory, National Institute of Genomic Medicine, Mexico City 14610, Mexico

Abstract. Cancer is a multifactorial disease characterized by the loss of control in the expression of genes known as cancer driver genes. Cancer driver genes trigger uncontrolled cell replication, which leads to the development of malignant tumors. A cluster of signal transduction pathways that contain cancer driver genes involved in cellular processes, such as cell proliferation, differentiation, apoptosis and dysregulated organ growth, are associated with cancer initiation and progression. In the present study, three signal transduction pathways involved in cervical cancer (CC) development were analyzed: The Hippo pathway (FAT atypical cadherin, yes-associated protein 1, SMAD4 and TEA domain family member 2), the Notch pathway [cellular-MYC, cAMP response element-binding binding protein (CREBBP), E1A-associated cellular p300 transcriptional co-activator protein and F-Box and WD repeat domain containing 7] and the nuclear factor erythroid 2-related factor 2 (NRF2) pathway [NRF2, kelch-like ECH-associated protein 1 (KEAP1), AKT and PIK3-catalytic subunit α]. Tumor samples from patients diagnosed with various stages of CC, including cervical intraepithelial neoplasia (CIN) 1, CIN 2, CIN 3, *in situ* CC and invasive CC, were analyzed. The mRNA expression levels were analyzed using reverse transcription-quantitative PCR assays, whereas protein expression levels were assessed through immunohistochemical tissue microarrays. High mRNA expression levels of c-MYC and AKT and low expression levels of NRF2 and KEAP1 were associated with a decreased survival time of patients with CC. Additionally, increased expression levels of c-MYC were detected in the invasive CC stage. At the protein level, increased NRF2 expression levels were observed in all five stages of CC samples compared with those in the cancer-free control samples. AKT1 was found to be dysregulated in the CIN 1 and CIN 2 stages, PI3K in the *in situ* and invasive stages, and CREBBP in the CIN 3 and *in situ* stages. In summary, the present study demonstrated significant changes in proteins of the Notch and NRF2 pathways in CC. NRF2 was overexpressed in all cervical cancer stages (cervical intraepithelial neoplasia, *in situ* CC and invasive CC). The present study makes an important contribution to the possible biomarker proteins to be analyzed for the presence of premalignant and malignant lesions in the cervix.

Introduction

The International Agency for Research on Cancer of the World Health Organization ranked cervical cancer (CC) fourth in terms of global incidence and third in terms of cancer-associated deaths among women in 2022, with 662,301 new cases and 348,874 associated deaths reported. Of these cases and deaths, 90% were reported from low- to middle-income countries (1).

There are numerous factors involved in the emergence and progression of CC. The most notable is persistent infection with the human papillomavirus (HPV). Additional factors include a compromised immune system, spontaneous mutations and lifestyle-related factors, such as smoking, alcohol consumption, hormonal therapies, malnutrition and a sedentary lifestyle, as well as vaginal dysbiosis associated

Correspondence to: Dr Gretel Mendoza-Almanza, Epigenetics Laboratory, National Institute of Genomic Medicine, 4809 Periferico Sur, Arenal Tepepan, Tlalpan, Mexico City 14610, Mexico
E-mail: gmendoza@inmegen.edu.mx

with *Sneathia* sp., *Fusobacterium* sp., *Pseudomonas* sp., *Streptococcus sp.,* human immunodeficiency virus and *Chlamydia* sp. (2), and mutations in cancer-driver genes, which can initiate carcinogenesis and promote disease progression by acting directly or influencing the activity of other genes (3). The IntOgen database, updated to 2023, provides valuable information on cancer driver genes and their pathways. Through the analysis of 266 cohorts comprising 33,019 samples across 73 types of cancer, the IntOgen database has classified 619 cancer driver genes. These findings highlight the broad impact and diversity of cancer driver genes in cancer research (4). The IntOGen database has analyzed four cohorts of patients with cervical squamous cell carcinoma, comprising 467 samples in total. The CC cohorts present with 9,749,109 mutations and 44 mutated cancer driver genes, including PIK3-catalytic subunit a (PI3KCA), FAT atypical cadherin (FAT1), SMAD4, F-Box And WD repeat domain containing 7 (FBXW7), kelch-like ECH-associated protein 1 (KEAP1), E1A-associated cellular p300 transcriptional co-activator protein (EP300), AKT1 and nuclear factor erythroid 2-related factor 2 (NRF2). Cellular-MYC (c-MYC) and cAMP response element-binding binding protein (CREBBP), are not reported as driver genes in CC, but are in other types of cancer. Examples for c-MYC include Burkitt's lymphoma, malignant lymphoma and acute myeloid leukemia, while examples for CREBBP include bladder urothelial carcinoma, non-small cell lung cancer, ovarian epithelial tumor and hepatocellular carcinoma (4). Yes-associated protein 1 (YAP1) and TEA domain family member 2 (TEAD2) have not been reported as driver genes.

The NRF2 pathway is a detoxifying pathway activated by high levels of ROS. The NRF2 and KEAP1 genes form a complex where KEAP1 anchors to the cytoskeleton. When the KEAP1-NRF2 link is lost, NRF2 can relocate to the nucleus and activate the transcription of genes necessary to eliminate toxins within the cell. The NRF2 pathway inhibits the development of multiple diseases, including cancer and neurodegenerative diseases (5). However, in addition to the protective role of NRF2 in normal cells, its role in cancer cells has also been highlighted, where aberrant signal transduction in the NRF2 pathway leads to the constitutive activation of NFE2L2 and thereby the positive regulation of its target genes, promoting cell survival (6). Dual activity of NFE2L2 has been observed in various cancer types, where its overactivation induces the expression of genes that allow tumor cells to acquire altered survival capabilities through mechanisms such as self-renewal capacity and repression of apoptosis (6).

The Notch pathway is involved in cellular differentiation and embryonic development, but has also been identified as hyperactive in cancer (7). c-Myc, the most studied proto-oncogene of the Myc family, is altered in various solid tumors, leukemias and lymphomas, and is involved in functions such as cell differentiation, cell adhesion, migration and angiogenesis, among others (8).

Finally, the Hippo signaling pathway is a kinase cascade that recognizes FAT1 as the primary initiator of the pathway. Under normal conditions, its leading role is to promote cell death and differentiation, and inhibit proliferation. Therefore, this pathway regulates cell fate, differentiation and organ growth (9).

The present study aimed to analyze the aforementioned genes in the different stages of CC, which are classified according to the cervical epithelial abnormalities caused by the presence of HPV in cervical intraepithelial neoplasia (CIN) 1, the earliest form of precancerous lesions. CIN 2 and CIN 3 are grouped as high-grade squamous intraepithelial lesions. The last group is the cervical cancerous stages known as *in situ* and invasive CC (10).

All the genes analyzed in the present study are involved in signaling pathways closely related to cancer development and are mostly cancer-driver genes (11). The identification of driver genes and understanding their roles in cancer development is crucial for the development of targeted therapies and personalized treatment strategies for patients with cancer.

Materials and methods

Ethics statement. The present study used formalin-fixed, paraffin-embedded (FFPE) cervical tissue, as approved by the Research Ethics Committee of the General Hospital Zacatecas 'Luz Cosío González', (Mexico City, Mexico; approval no. 0131/2018). The FFPE cervical tissue samples used were ≥10 years old from the Department of Pathology hospital archive; therefore, the requirement for patient consent was waived. All protocols were designed and performed according to the principles of the Declaration of Helsinki.

FFPE cervical tissue. Patients were previously diagnosed at the Department of Pathology, General Hospital Zacatecas 'Luz González Cosío', and their samples divided into the following groups: Non-precancerous or non-cancerous tissue (control), CIN 1, CIN 2, CIN 3, *in situ* CC or invasive CC. For the reverse transcription-quantitative PCR (RT-qPCR) assays, a total of 81 samples were analyzed, which consisted of 12 control cervical tissue (non-neoplastic), 16 CIN 1 samples, 14 CIN 2 samples, 12 CIN 3 samples, 18 samples of *in situ* CC and 9 samples of invasive CC. For the immunohistochemistry (IHC) analyses in tissue microarrays (TMAs), 159 independent samples were examined, including 24 samples of non-neoplastic cervical tissue, 42 CIN 1 samples, 33 CIN 2 samples, 16 CIN 3 samples, 32 *in situ* CC samples and 12 samples of invasive CC. The inclusion criteria for both patient sample cohorts were: i) Sufficient quantity of fixed tissue; and ii) sufficient RNA, in the case of the RT-qPCR assays. The sample exclusion criteria were: i) Insufficient quantity of malignant tissue; and ii) insufficient RNA, in the case of the RT-qPCR assays.

Gene expression analysis
RNA extraction from FFPE tissue samples. From each FFPE cervical tissue sample, 10 sections of 5 μm in thickness were obtained using a microtome. Tissue sections were deparaffinized at 37˚C through washes with xylene for 1 h and 96 and 70% ethyl alcohol for 5 min for each wash. RNA extraction was carried out using TRIzol™ (cat. no. 15596018; Thermo Fisher Scientific, Inc.), according to the manufacturer's protocol for RNA extraction in mammalian cells, with minor modifications. A total of 500 μl proteinase K buffer [50 mM Tris (pH 8.0), 400 mM NaCl, 2 mM EDTA and 4% SDS] and 50 μl of 20 mg/ml proteinase K were added to the deparaffinized samples and incubated overnight, with 400-rpm agitation at

50˚C. The next day, samples were incubated for 1 h at 90˚C without agitation to break the cross-linkage between nucleic acids and proteins, to release the nucleic acids (12). Following this, the manufacturer's protocol for RNA extraction in mammalian cells was continued. The concentration and purity of the extracted RNA were determined using a NanoDrop™ One Spectrophotometer (Thermo Fisher Scientific, Inc.). The extracted RNA was subsequently used for the synthesis of cDNA.

Synthesis of cDNA. DNA decontamination was performed on the extracted RNA through digestion with the DNase I, RNase-free kit (1 U/μl) (cat. no. EN0521; Thermo Fisher Scientific, Inc.), according to the manufacturer's instructions. The concentration and purity of the decontaminated DNA were measured using a NanoDrop One Spectrophotometer (Thermo Fisher Scientific, Inc.). cDNA synthesis was performed using the SuperScript™ IV Reverse Transcriptase kit (cat. no. 18090200; Thermo Fisher Scientific, Inc.), following the manufacturer's instructions, with some modifications. Random hexamers (50 ng/μl; cat. no. C118A; Promega Corporation) were added and incubated at 70˚C for 10 min, followed by incubation at 45˚C for 5 min. Next, the RT SuperScript 5X Buffer, DTT (100 nM), dNTPs (10 mM), RNase inhibitor RiboLock (40 U/μl) and RT SuperScript enzyme (200 U/μl) were added, followed by overnight incubation at 45˚C (13). The next day, samples were incubated for 10 min at 70˚C. The newly synthesized cDNA was stored at -70˚C until use.

qPCR. The qPCR mix contained cDNA from each sample, primers (10 pmol of each primer), water and Maxima™ SYBR® Green/ROX qPCR Master Mix (cat. no. K0222; Thermo Fisher Scientific, Inc.). The qPCR was performed using the QuantStudio 1™ Real-Time PCR system (cat. no. A40426; Thermo Fisher Scientific, Inc.). The following thermocycling conditions were used for PCR: 50˚C for 2 min, 95˚C for 10 min, and 40 cycles of 95˚C for 15 sec and 57.5˚C for 1 min. Primer sequences were designed using the mRNA sequence for each gene as reported in the National Center for Biotechnology Information database (https://www.ncbi.nlm.nih.gov/nucleotide/) (Table I). The relative expression of each gene was determined using the $2^{-\Delta\Delta Cq}$ method (14), normalized to GAPDH gene expression. Samples with a Cq value >39 were discarded.

Protein expression analysis
TMA construction. A total of 159 FFPE samples from various stages of CC were selected, including non-lesioned, precancerous and cancerous samples, and analyzed for TMA construction. Each tissue sample had been previously examined using hematoxylin and eosin staining to define the diagnostic areas. The selected tissues were punched with a 1-mm needle and transferred onto a recipient paraffin block using a Chemicon Advanced Tissue Arrayer ATA100 (Chemicon International; Thermo Fisher Scientific, Inc.). Tissue sections of 5 μm in thickness were cut from each TMA and placed onto positively charged slides (VWR Superfrost Plus; VWR International; Avantor, Inc.).

IHC analysis on TMA. Protein expression analysis was performed using IHC on the TMA. The following primary antibodies were used at a 1:50 dilution: NRF2 (cat. no. Y414975),

KEAP1 (cat. no. Y400489), PIK3CA (cat. no. Y011508), AKT (cat. no. Y409091), SMAD4 (cat. no. Y401229), CMYC (cat. no. Y080045) and CREBBP (cat. no. Y401909) (all Applied Biological Materials, Inc.), FAT1 (cat. no. NBP1-84565; Novus Biologicals, Ltd.; Bio-Techne) and TEAD2 (cat. no. AB273017; Abcam). Protein expression levels were detected using the DAB HRP Brown IHC detection system from Bio SB, Inc., following the manufacturer's protocol. The slides were imaged using the Aperio LV1-Real-time Digital Pathology System (Leica Biosystems), and tissue images were analyzed using the Aperio ImageScope software (version 12.3.3.5048; Leica Biosystems).

Image analysis. The expression levels of each protein in the tumor fraction of the samples within the microarray were assessed using a semi-quantitative method involving visual analysis. A numerical score was assigned to: i) The intensity of staining (intensity); and ii) the proportion of positive cells showing expression of the protein of interest (positivity). A visual appraisal was conducted, in which three independent expert evaluators, in a blinded analysis, assigned scores from 0 to 3 as follows: No staining, 0; weak staining, 1; moderate staining, 2; and intense staining, 3, which reflected the percentage of expression from 0-100%. Scores from 1 to 4 were also assigned as follows: 0-25% Tissue expression, 1; 26-50% expression, 2; 51-75% expression, 3; and 76-100% expression, 4, reflecting the percentage of positivity from 0-100% (Fig. 1). The proteins of interest were assessed in each of the tumors from cervical cancer patients, analyzing their expression intensity categorized as high, medium, low or absent, reflected on a scale from 0 to 3.

Statistical analysis. The data generated were analyzed for normality using the Shapiro-Wilk test. Subsequently, a comparative analysis of relative expression levels among the different groups was conducted using the Kruskal-Wallis test, followed by the Dunn multiple comparisons test. P<0.05 was considered to indicate a statistically significant difference. P<0.05 was used to indiciate a statistically significant difference. Statistical analysis was performed using GraphPad Prism software (version 9.0; Dotmatics).

Bioinformatic analysis
Kaplan-Meier plots. Analysis was conducted using data retrieved from the Kaplan-Meier plotter platform (https://www.kmplot.com/analysis/) (15), with the following parameters: Pan-Cancer RNA-seq generated database, patients stratified by median age, automatic selection of the best cut-off value, overall survival and no restriction by cancer stage or cellular content.

Search Tool for Retrieval of Interacting Genes/Proteins (STRING). The analysis of protein-protein interaction networks and functional enrichment analysis was performed using a STRING Core Data Resource version 12.0 (https://string-db.org) with the following parameters: Full STRING network; type of interaction, evidence; and interaction source, experiments, database, co-occurrence and co-expression (16). The cellular processes were analyzed within which the aforementioned selected genes were involved (Table II).

Table I. Sequences of primers used for reverse transcription-quantitative PCR.

Gene	NCBI accession no.	Sequence (5'-3')
FAT1	NM_005245.4	F: TTCAAAATAGGTGAAGAGACAGGTG
		R: TTGTGATGAGACCTGTTTTAGGATG
YAP1	NM_001195045.2	F: GCCCACTCGGGATGTAACTT
		R: AACCCTTTGGTCTCCGACAG
TEAD2	NM_001256658.2	F: GTAGAGTTCTCAGCCTTCGTG
		R: ATTTGTCGTAGATCTGCCGG
SMAD4	NM_005359.6	F: GAGGTTATGGTTCTGGGTGG
		R: GAAAGGCACTGGACAAACATG
NRF2	NM_006164.5	F: ATAGCTGAGCCCAGTATC
		R: CATGCACGTGAGTGCTCT
KEAP1	NM_203500.2	F: CCGGGAGTACATCTACATGC
		R: TGATGCAGGCGTGGAAG
PIK3CA	NM_006218.4	F: TGGTTAAAGATCCAGAAGTACAGG
		R: TTTGGCAATTCTGGTGAAGATTC
AKT 1	NM_005163.2	F: GCTGAAGAGATGGAGGTGTC
		R: AGGATCACCTTGCCGAAAG
MYC	NM_002467.6	F: AATGAAAAGGCCCCCAAGGTAGTTATCC
		R: GTCGTTTCCGCAACAAGTCCTCTTC
CREBBP	NM_004380.3	F: TCAAACCCCAGTTCAGCC
		R: AGGGACTCTGTTATCAATGCTG
EP300	NM_001429.4	F: GTGAACTCTCCTATAATGCCTCC
		R: ATGAAGAGCTGGTTGAGGAAG
FBXW7	NM_033632.3	F: AAAGAGTTGTTAGCGGTTCTCG
		R: CCACATGGATACCATCAAACTG
GAPDH	NM_002046.7	F: CACCATGGAGAAGGCTGG
		R: TGCTGATGATCTTGAGGCTG

NCBI, National Center for Biotechnology Information; F, forward; R, reverse; PI3KCA; PIK3-catalytic subunit a; FAT1, FAT atypical cadherin; FBXW7, F-Box And WD repeat domain containing 7; KEAP1, kelch-like ECH-associated protein 1; EP300, E1A-associated cellular p300 transcriptional co-activator protein; NRF2, nuclear factor erythroid 2-related factor 2; c-MYC, cellular-MYC; CREBBP, cAMP response element-binding binding protein; YAP1, yes-associated protein 1; TEAD2, TEA domain family member 2.

Results

Protein expression and protein interactions. The present study analyzed the expression of transcripts and proteins of 12 genes related to the Notch, Hippo and NRF2 signal transduction pathways. Fig. 1 summarizes the cellular positivity and intensity in the expression found in precancerous lesions, cancerous lesions and control cervical tissue through immunohistochemistry assays for the proteins analyzed.

To investigate the relationship between gene expression and CC, the protein-protein interactions of three critical molecular nodes, namely the Hippo, Notch and NRF2 pathways, were analyzed (Fig. 2).

The STRING analysis showed that the Hippo pathway had a close association with genes within the SMAD and TEAD families (Fig. 2A). It was demonstrated that the SMAD family is linked to the Notch pathway through TGF-β, a crucial pathway in cancer development (17).

Through gene interaction analysis using the STRING platform, it was demonstrated that Notch pathway associations belonged to MYC pathway genes, such as EP300, FBXW7,

CREBBP, TL2, TL3, TCF7L1 and MAML3 (Fig. 2B). By contrast, CREBBP mainly networked with EP300, CREB3L4, CREB3, CREB3L2, CITED2 and CITED1. Additionally, FBXW7 interacted with CREBBP, EP300, MAML2, RBPJ and MAML3. Moreover, EP300 was associated with CREB3, CREB3L2, RBPJL, MAML1, MAML1, TLE3, TL2 and CITED2. In summary, a large majority of the genes resulting from the present interaction analyses were associated with carcinogenesis and cell proliferation (18).

The NRF2/KEAP1 axis establishes crosstalk with the PI3K/AKT1 axis in cellular detoxification through reactive oxygen species (ROS) (19). These axes converged through the direct interaction of AKT and NRF2 (Fig. 2C). In this context, the interactions of genes that belong to the selected nodes of interest with other proteins were recreated from known significative interactions, such as PIK3CA with PDPK1, AKT1 and AKT3, known for their oncogenic activity and promotion of tumor growth (18). AKT, by contrast, serves a vital role in cancer development and progression through interactions with NRF2, PIK3CA, PDPK1 and AKT2. NRF2 directly interacted with KEAP1, AKT1, AKT2, AKT3, critical genes that regulate
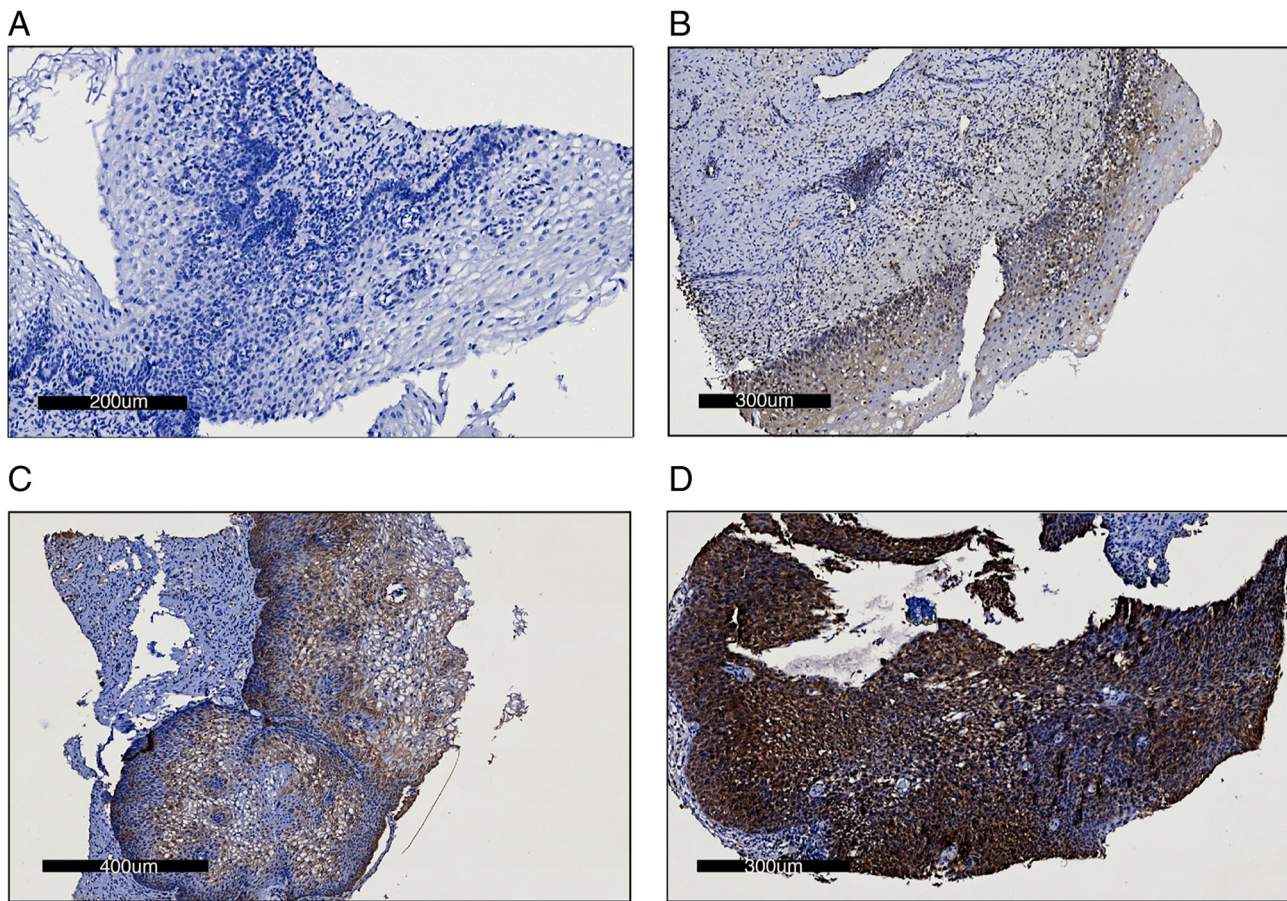
Figure 1. Immunohistochemistry images of the staining intensity of cervical cancer tumor samples. Representative images of (A) no staining, assigned 0 points (scale bar, 200 nm), (B) weak staining, assigned 1 point (scale bar, 300 nm), (C) moderate staining, assigned 2 points (scale bar, 400 nm) and (D) intense staining, assigned 4 points (scale bar, 300 nm).

tumorigenesis and cancer progression (17). Furthermore, KEAP1 interacted with DPP3, ENC1 and NRF2.

Hippo pathway in CC. To investigate the relevance of these signaling nodes, survival rates among patients with CC associated with the expression levels of each aforementioned gene were explored. The mRNA and protein expression levels were assessed in tissue samples obtained from patients diagnosed with CIN 1, 2 and 3, *in situ* CC and invasive CC, using cervical tissue samples without neoplasia as a control for expression levels (Figs. 3-5).

The Hippo pathway is a cascade of serine/threonine kinases that serves a role in organ growth, survival and differentiation (9). A recent study showed that dysregulation of the Hippo pathway was associated with the onset of certain types of cancer (20). Analysis was conducted of four molecules of the Hippo pathway, namely FAT1, YAP1, SMAD4 and TEAD2, in samples from patients with CC.

Kaplan-Meier curves demonstrated positive hazard ratio (HR) values for the high expression groups of the four genes, YAP1 (HR, 2.13), FAT1 (HR, 2.07), TEAD2 (HR, 1.7), SMAD 4 (HR, 1.48) and which indicated lower survival rates within the first 60 months from diagnosis (Fig. 3A, E, G and K). This suggested that a lower survival rate was associated with high mRNA expression levels of the genes involved in the Hippo pathway. However, no significant differences in the mRNA

expression levels of FAT1, YAP1, SMAD4 and TEAD2 were identified, potentially due to the dispersion of values in these Hippo pathway genes, although a notable increase in expression levels in invasive CC samples was observed compared with those in the control (Fig. 3B, F, H and L). At the protein level, there was no significant difference in the percentage of cells expressing the Hippo pathway proteins nor in the intensity in CC samples when compared with the control sample group or between different stages of CC (Fig. 3C, D, I, J, M and N).

Notch pathway in CC. The Notch pathway is a highly conserved cell signaling system in a large proportion of multicellular organisms (21); it is crucial in various cellular processes, including cell proliferation, differentiation and apoptosis. Dysregulation of the Notch pathway has been implicated in numerous human diseases, including cancer (22). Analysis of four proteins from the Notch pathway was conducted, namely c-MYC, CREBBP, EP300 and FBXW7, in tissue samples from patients with different stages of CC. The analysis demonstrated an HR of 1.95 for c-MYC, which suggested that patients with high expression levels of c-MYC have a lower survival rate up to 60 months (Fig. 4). However, EP300, CREBBP and FBXW7 showed HR values of 0.55, 0.6 and 0.6 respectively, which suggested that patients with CC with high levels of these proteins have a slight increase in survival rate at 60 months (Fig. 4A, E, I and K).

Table II. Inference of potentially dysregulated cellular processes[a].

Term ID, GO no.	Term description	Observed gene count, n	Background gene count, n	Strength[b]	False discovery rate[c]	Matching proteins in the network
0009628	Response to abiotic stimulus	5	1,107	1.25	0.0038	CREBBP, PIK3CA, NRF2, AKT1 and c-MYC
0002682	Regulation of immune system process	5	1,438	1.14	0.0073	CREBBP, PIK3CA, NRF2, AKT1 and c-MYC
0042592	Homeostatic process	5	1,406	1.15	0.0073	CREBBP, PIK3CA, NRF2, AKT1 and c-MYC
0009966	Regulation of signal transduction	5	2,978	0.82	0.0314	CREBBP, PIK3CA, NRF2, AKT1 and c-MYC
0031325	Positive regulation of cellular metabolic process	5	3,114	0.8	0.0361	CREBBP, PIK3CA, NRF2, AKT1 and c-MYC
0051173	Positive regulation of nitrogen compound metabolic process	5	3,166	0.79	0.0373	CREBBP, PIK3CA, NRF2, AKT1 and c-MYC
0006950	Response to stress	5	3,358	0.77	0.0428	CREBBP, PIK3CA, NRF2, AKT1 and c-MYC
0010604	Positive regulation of macromolecule metabolic process	5	3,533	0.75	0.0442	CREBBP, PIK3CA, NRF2, AKT1 and c-MYC
0036293	Response to decreased oxygen levels	4	291	1.73	0.0038	CREBBP, NRF2, AKT1 and c-MYC
0080135	Regulation of cellular response to stress	4	712	1.35	0.012	CREBBP, NRF2, AKT1 and c-MYC
0043066	Negative regulation of apoptotic process	4	891	1.25	0.0218	PIK3CA, NRF2, AKT1 and c-MYC
0045944	Positive regulation of transcription by RNA polymerase II	4	1,250	1.1	0.0314	CREBBP, NRF2, AKT1 and c-MYC
0051247	Positive regulation of protein metabolic process	4	1,512	1.02	0.0428	PIK3CA, NRF2, AKT1 and c-MYC
0033554	Cellular response to stress	4	1,572	1	0.0442	PIK3CA, NRF2, AKT1 and c-MYC
0036294	Cellular response to decreased oxygen levels	3	136	1.94	0.0089	NRF2, AKT1 and c-MYC
0009411	Response to UV	3	150	1.9	0.0089	CREBBP, AKT1 and c-MYC
2001242	Regulation of intrinsic apoptotic signaling pathway	3	169	1.84	0.0102	NRF2, AKT1 and c-MYC
0071375	Cellular response to peptide hormone stimulus	3	240	1.69	0.0102	PIK3CA, NRF2 and AKT1
0062197	Cellular response to chemical stress	3	272	1.64	0.0218	PIK3CA, NRF2 and AKT1
0001666	Response to hypoxia	3	278	1.63	0.0229	CREBBP, NRF2 and c-MYC
0043276	Anoikis	2	22	2.82	0.0232	PIK3CA and AKT1

Table II. Continued.

Term ID, GO no.	Term description	Observed gene count, n	Background gene count, n	Strength[b]	False discovery rate[c]	Matching proteins in the network
1902176	Negative regulation of oxidative stress-induced intrinsic apoptotic signaling pathway	2	26	2.64	0.0102	NRF2 and AKT1
0044030	Regulation of DNA methylation	2	25	2.5	0.0128	PIK3CA and c-MYC
0034405	Response to fluid shear stress	2	34	2.97	0.0218	NRF2 and AKT1
0016242	Negative regulation of macroautophagy	2	35	2.35	0.0254	PIK3CA and AKT1
0046326	Positive regulation of glucose import	2	36	2.34	0.0255	NRF2 and AKT1
0031295	T cell co-stimulation	2	42	2.27	0.0272	PIK3CA and AKT1
0035924	Cellular response to vascular endothelial growth factor stimulus	2	42	2.27	0.0272	PIK3CA and AKT1
0043491	Phosphatidylinositol 3-kinase/protein kinase B signal transduction	2	49	2.24	0.0272	PIK3CA and AKT1
0007173	Epidermal growth factor receptor signaling pathway	2	49	2.21	0.0235	PIK3CA and AKT1
0043491	Phosphatidylinositol 3-kinase/protein kinase B signal transduction	2	53	2.17	0.0814	PIK3CA, AKT1
0043536	Positive regulation of blood vessel endothelial cell migration	2	53	2.17	0.0814	NRF2 and AKT1
0008286	Insulin receptor signaling pathway	2	64	2.09	0.0979	PIK3CA and AKT1
0006112	Energy reserve metabolic process	2	66	2.08	0.0873	AKT1 and c-MYC
0043542	Endothelial cell migration	2	69	2.06	0.0994	PIK3CA and AKT1
0048661	Positive regulation of smooth muscle cell proliferation	2	85	1.97	0.0412	PIK3CA and AKT1
0036294	Cellular response to decreased oxygen levels	3	135	1.94	0.0089	NRF2, AKT1 and c-MYC
0034644	Cellular response to UV	2	30	1.94	0.0459	CREBBP and c-MYC
2000777	Positive regulation of proteasomal ubiquitin-dependent protein catabolic process involved in cellular response to hypoxia	2	50	1.91	0.0412	NRF2 and AKT1
0009411	Response to UV	3	150	2.0	0.0102	CREBBP, AKT1 and c-MYC

[a]Created in STRING function network Version 12.0. [b]Log10 (observed/expected) annotations. [c]P-values corrected for multiple testing within each category using the Benjamini-Hochberg procedure. ID, identification; GO, Gene Ontology; PI3KCA, PIK3-catalytic subunit a; NRF2, nuclear factor erythroid 2-related factor 2; c-MYC, cellular-MYC; CREBBP, cAMP response element-binding binding protein.
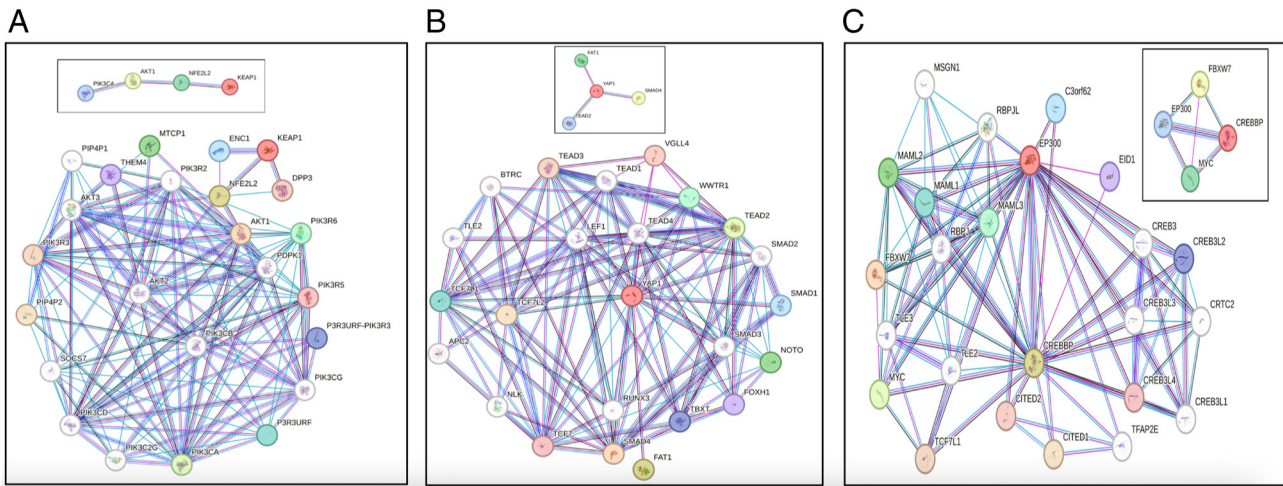
Figure 2. Protein-protein interaction networks. (A) Protein-protein interactions of the Hippo pathway. (B) Protein-protein interaction of the Notch pathway. (C) Protein-protein interactions of the NRF2/KEAP1 and PIK3CA/AKT pathways. The inset image depicts interactions between the proteins analyzed in the present study from each pathway (Notch, Hippo and NRF2). The larger boxed image depicts interactions with 20 proteins. The colored lines represent the interaction source as follows: Experiments, pink; database, aqua blue; co-occurrence, navy blue; and co-expression, black. Created in STRING function network (version 12.0). NRF2, nuclear factor erythroid 2-related factor 2; KEAP1, kelch-like ECH-associated protein 1; PIKCA, PIK3-catalytic subunit a.

Analysis of the mRNA expression levels of c-MYC showed a significant increase in expressions levels in the invasive stage of CC compared with the control group and with the other genes analyzed in this pathway (Fig. 4B, F, J and L). At the protein level, no significant difference in either the percentage of positivity or intensity staining was detected (Fig. 4C and D); however, a significant increase in the protein intensity of CREBBP in the CIN 3 and *in situ* stages of CC was demonstrated (Fig. 4F-H).

NRF2 pathway in CC. NRF2 is a protein encoded by the NFE2L2 gene. NRF2 is a crucial regulator of the body's antioxidant response, as it is involved in cellular defense mechanisms against oxidative stress and inflammation (23,24). However, NRF2 signaling disruption has been implicated in a number of diseases, including cancer (25). In the present study, analysis of PI3K, AKT, NRF2 and KEAP1 as NRF2 pathway components in patients with CC was conducted.

Survival analyses indicated that a number of proteins associated with the NRF2 pathway exhibited a HR <1, including NRF2 (HR, 0.39; Fig. 5A), KEAP1 (HR, 0.41; Fig. 5E) and PI3K (HR, 0.65; Fig. 5I). This indicated that patients with elevated mRNA expression levels of these proteins showed an increased survival rate. By contrast, the AKT1 protein survival curve exhibited an HR of 2.02, which suggested that patients with high AKT1 expression levels had a lower survival probability at 60 months (Fig. 5A). However, analysis of mRNA expression levels of all four proteins demonstrated no significant differences when comparing CC with the control groups. Analysis of protein expression levels, however, demonstrated increased positivity of PI3KCA in CIN 2, *in situ* and invasive CC, while shown increased intensity in CIN 1, CIN 2, *in situ* and invasive CC. Significantly increased AKT1 protein expression intensity was found in the CIN 1 and CIN 2 stages of CC. Furthermore, NRF2 exhibited protein upregulation in all tumor samples, regardless of stage.

A summary analysis of the cellular processes potentially affected by the proteins c-Myc, CREBBP, PI3K, AKT1 and NRF2, which are dysregulated in patients with CC, was conducted (Fig. 6A). c-MYC from the Notch pathway showed an HR of 2.00 on Kaplan-Meier analysis. AKT1 from the NRF2 pathway showed an HR of 1.70, while NRF2 and KEAP1 from the same pathway exhibited the lowest HR of 0.39 and 0.41, respectively (Fig. 6B). Analysis of the mRNA and protein expression levels of the 12 proteins showed that NRF2 protein expression levels measured by IHC were increased in all cancer groups, regardless of stage. AKT1 was upregulated in the CIN 1 and CIN 2 stages, and PI3K in the CIN 2, *in situ* and invasive stages of CC. Moreover, mRNA expression levels of c-MYC from the Notch pathway were also increased at the invasive stage, while CREBBP protein was downregulated in the CIN 3 and *in situ* stages of CC. Bioinformatic analysis indicated the cellular processes in which these five dysregulated proteins may be involved, among which responses to abiotic stimuli, regulation of the immune system and homeostasis maintenance were identified. Through analysis of the modified processes according to their strength, which according to STRING, is a measure Log10 (observed/expected) that describes how large the enrichment effect is. The present results showed that even without involvement of the aforementioned five genes, the main processes involved were 'anoikis' with the participation of two proteins (PIK3CA and AKT1), and 'negative regulation of oxidative stress-induced intrinsic apoptotic signaling pathway' (NRF2 and AKT1) (Table II).

Discussion

Cancer arises from genetic alterations, which can be either hereditary or induced by an individual's lifestyle or environmental factors. These genetic alterations confer selective advantages to the emerging cancer cell clones, and enable them to resist apoptosis, achieve replicative immortality,
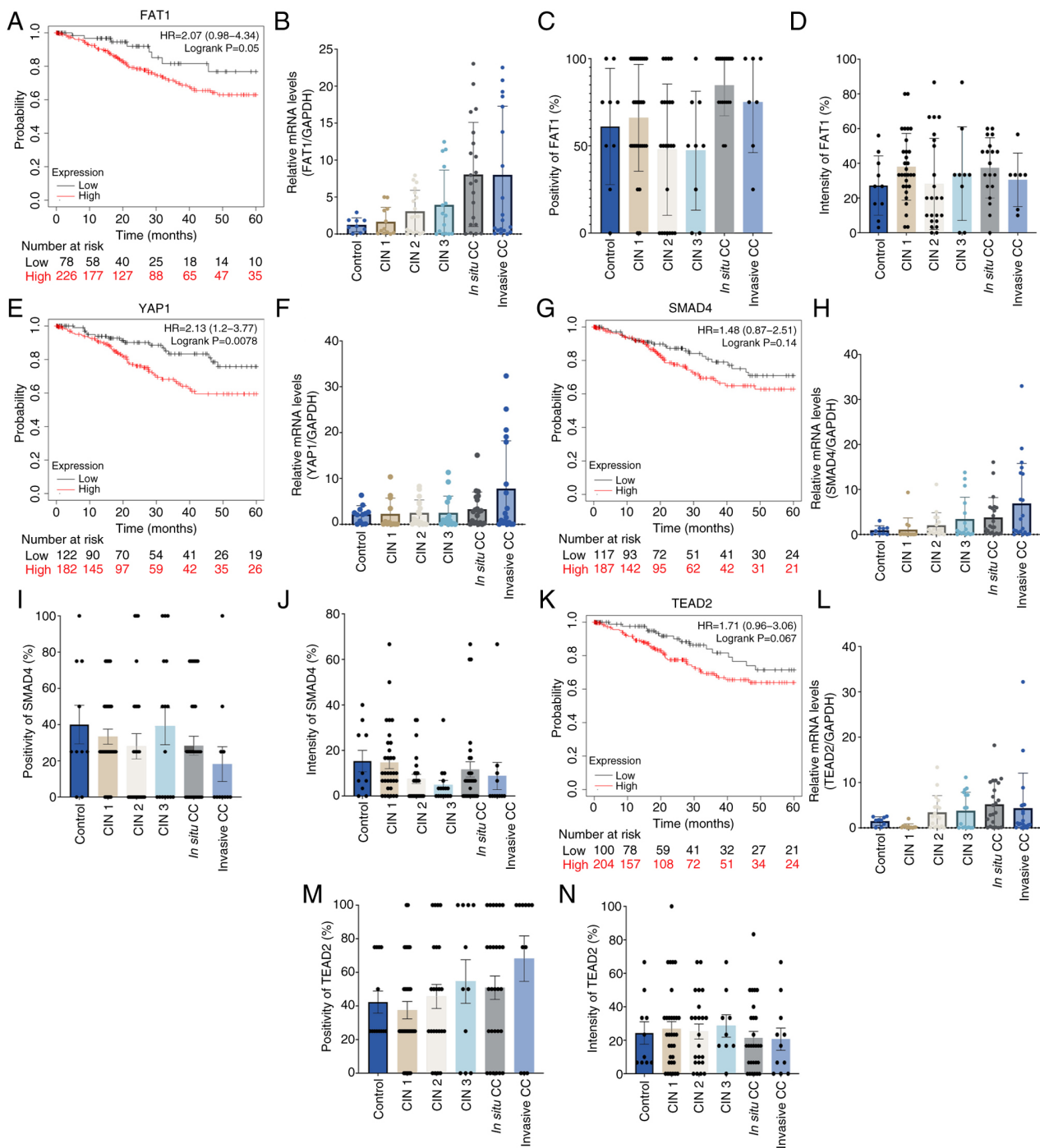
Figure 3. Hippo pathway gene expression analyses. (A) Survival analysis of patients with high and low expression levels of FAT1. (B) Relative expression levels of FAT1 in tumor samples from precursor stages to invasive carcinoma. IHC protein expression levels as quantified by (C) positive cells for FAT1 antibody staining and (D) the intensity of the cell response to the antibody. (E) Survival analysis of patients with high and low expression levels of YAP1. (F) Relative expression levels of YAP1 from precursor stages to invasive carcinoma. (G) Survival analysis of patients with high and low expression levels of SMAD4. (H) Relative expression levels of SMAD4 from precursor stages to invasive carcinoma. IHC protein expression levels as quantified by (I) positive cells for SMAD4 antibody staining and (J) the intensity of the cell response to the antibody. (K) Survival analysis of patients with high and low expression levels of TEAD2. (L) Relative expression levels of TEAD2 from precursor stages to invasive carcinoma. IHC protein expression levels as quantified by (M) positive cells for TEAD2 antibody staining and (N) the intensity of the cell response to the antibody. Error bars represent the standard deviation. HR, hazard ratio; CIN, cervical intraepithelial neoplasia; FAT1, FAT atypical cadherin; TEAD2, TEA domain family member 2; YAP1, yes-associated protein 1.

induce angiogenesis, activate invasion and metastasis, reprogram cellular metabolism, and evade growth-suppressing signals and the immune response (26). Additionally, the association of cancer cells with the tumor microenvironment promotes disease progression, tumor growth, angiogenesis and metastasis (27).

The genes analyzed in the present study are involved in the NRF2, Notch and Hippo pathways, which are a part of a cluster of pathways related to cancer development and progression that serve crucial roles in cellular processes, which makes them potential targets for the study of novel treatments and technological advances in diagnosis.
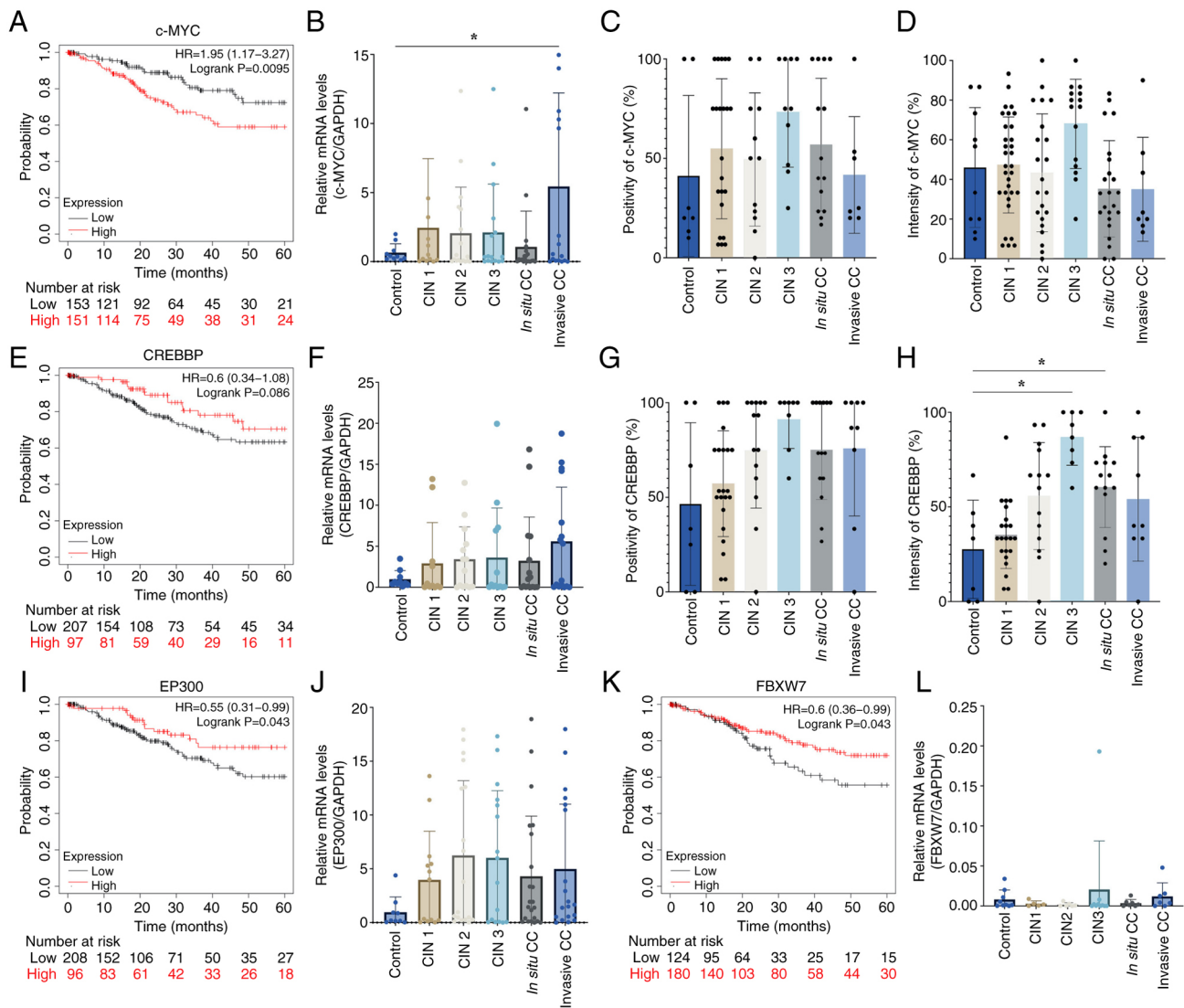
Figure 4. Notch pathway gene expression analyses. (A) Survival analysis of patients with high and low expression levels of c-MYC (B) Relative expression levels of c-MYC from precursor stages to invasive carcinoma. IHC protein expression levels as quantified by (C) positive cells for c-MYC antibody staining and (D) the intensity of the cell response to the antibody. (E) Survival analysis of patients with high and low expression levels of CREBBP. (F) Relative expression levels of CREBBP from precursor stages to invasive carcinoma. IHC protein expression levels as quantified by (G) positive cells for CREBBP antibody staining and (H) the intensity of the cell response to the antibody. (I) Survival analysis of patients with high and low expression levels EP300. (J) Relative expression levels of EP300 from precursor stages to invasive carcinoma. (K) Survival analysis of patients with high and low expression levels of FBXW7. (L) Relative expression levels of FBXW7 from precursor stages to invasive carcinoma. Error bars represent the standard deviation. *$P<0.05$. HR, hazard ratio; CIN, cervical intraepithelial neoplasia; c-MYC, cellular-MYC; CREBBP, cAMP response element-binding binding protein; EP300, E1A-associated cellular p300 transcriptional co-activator protein; FBXW7, F-Box and WD repeat domain containing 7.

Kaplan-Meier survival curve analyses suggested that the genes that provided more valuable information associated with survival were c-MYC from the Notch pathway, and NRF2, KEAP1 and AKT1 from the NRF2 pathway. This data demonstrated that patients with CC with high gene expression levels of c-MYC or AKT1; or low gene expression levels of NRF2 and KEAP1 have a decreased probability of survival.

Analysis of mRNA expression levels of the genes that form the three signal transduction pathways demonstrated that c-MYC mRNA provided relevant information regarding invasive CC samples. c-MYC is a widely studied proto-oncogene in solid tumors (28). Alterations in this gene have been demonstrated in patients who develop HPV-positive CC. Furthermore, the integration of HPV sequences near the c-MYC locus has been demonstrated in some cervical cell

lines and genital tumors, which suggests a synergistic role of HPV and the c-MYC proto-oncogene in CC development (29).

By contrast, CREBBP protein expression levels (Notch pathway) were increased in CIN 3 and *in situ* stages of CC in the present study. Limited information is available regarding the status of CREBBP in CC. However, this gene is known to be altered in at least 5% of cancer cases, with an increased prevalence of CREBBP mutations observed in breast, bladder, lung and colon cancer types (30,31). CREBBP contributes to tumor progression and to tumor microenvironment development (32); its role in transcriptional regulation involves serving as a scaffold between specific DNA regions and the transcription machinery, as well as in histone acetylation and interactions with transcription factors (33). CREBBP has a dual function; it binds
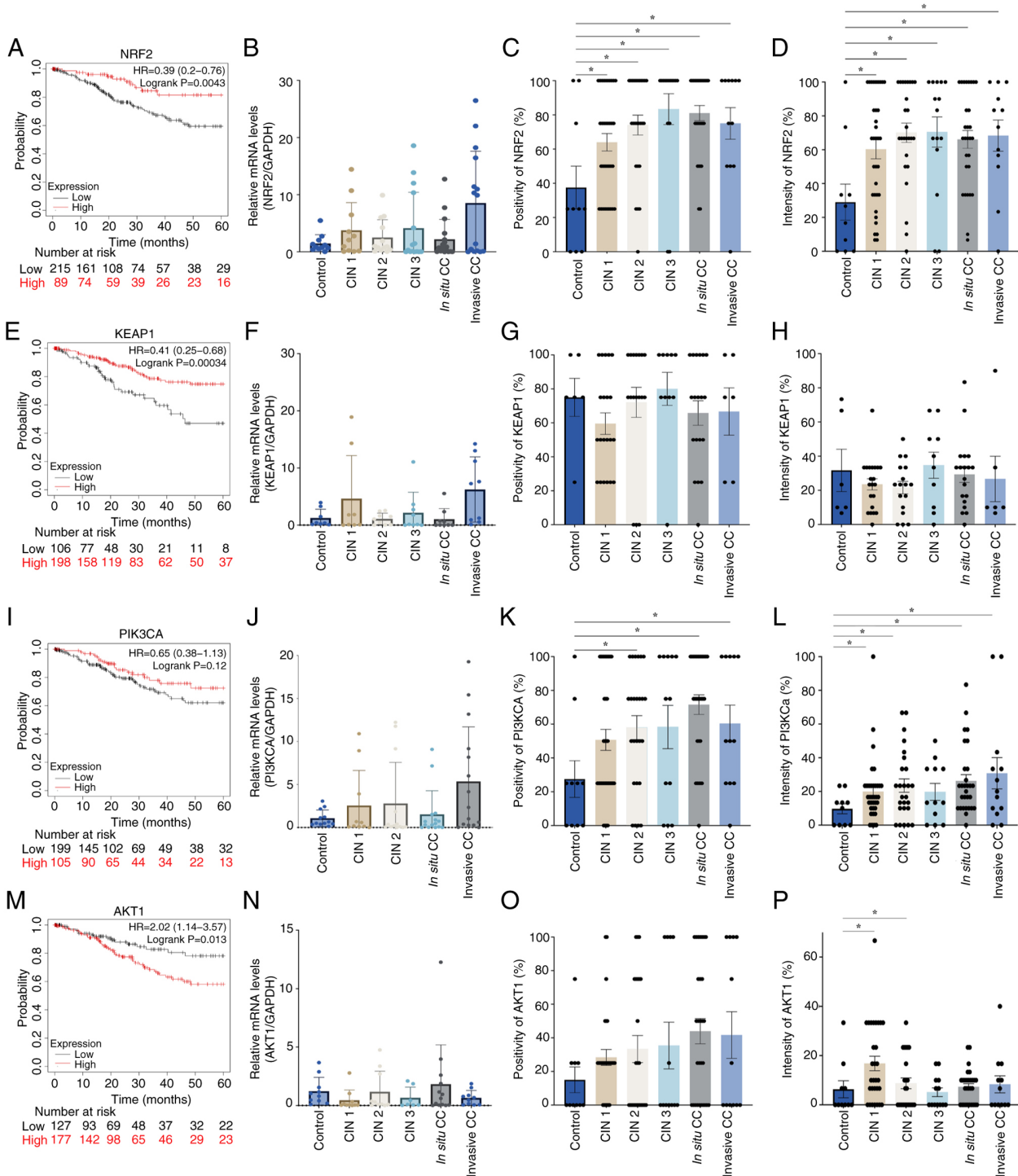
Figure 5. NRF2 pathway gene expression analyses. (A) Survival analysis of patients with high and low expression levels of NRF2. (B) Relative expression levels of NRF2 from precursor stages to invasive carcinoma. IHC protein expression levels as quantified by (C) positive cells for NRF2 antibody staining and (D) the intensity of the cell response to the antibody. (E) Survival analysis of patients with high and low expression levels of KEAP1. (F) Relative expression levels of KEAP1 from precursor stages to invasive carcinoma. IHC protein expression levels as quantified by (G) positive cells for KEAP1 antibody staining and (H) the intensity of the cell response to the antibody. (I) Survival analysis of patients with high and low expression levels of PI3K. (J) Relative expression levels of PI3K from precursor stages to invasive carcinoma. IHC protein expression levels as quantified by (K) positive cells for PI3K antibody staining and (L) the intensity of the cell response to the antibody. (M) Survival analysis of patients with high and low expression levels of AKT1. (N) Relative expression levels of AKT1 from precursor stages to invasive carcinoma. IHC protein expression levels as quantified by (O) positive cells for AKT1 antibody staining and (P) the intensity of the cell response to the antibody. Error bars represent the standard deviation. *P<0.05. HR, hazard ratio; CIN, cervical intraepithelial neoplasia; NRF2, nuclear factor erythroid 2-related factor 2; KEAP1, kelch-like ECH-associated protein 1; PI3KCA, PIK3-catalytic subunit α.

to transcription factors and associates them with larger molecular complexes. Additionally, as an acetyltransferase, the protein possesses transformative capabilities, primarily on histones, which promote chromatin accessibility (33). Further research is needed to understand CREBBP functions in CC.

A

PATHWAY	GENE	CIN 1	CIN 2	CIN 3	*In situ* CC	Invasive CC
NOTCH	c-MYC					mRNA
	CREBBP			% I	% I	
NRF2	PIK3CA	% P	% P, I		% P, I	% P, I
	AKT1	% P	% P			
	NRF2	% P, I	% P, I	% P, I	% P, I	% P, I

B

PATHWAY	mRNA	HR
HIPPO	YAP1	2.13
HIPPO	FAT1	2.07
NRF2	AKT1	2.02
NOTCH	c-MYC	1.95
HIPPO	TEAD2	1.71
HIPPO	SMAD4	1.48
NRF2	PIK3CA	0.65
NOTCH	CREBBP	0.6
NOTCH	FBXW7	0.6
NOTCH	EP300	0.55
NRF2	KEAP1	0.41
NRF2	NRF2	0.39

C
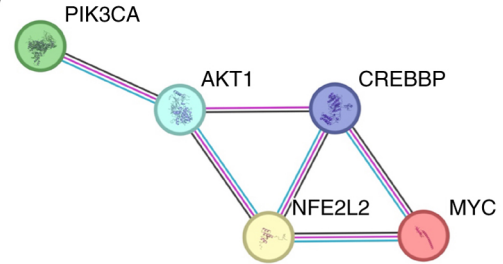
Figure 6. Integrated analysis of results of the present study. (A) Summary of HR values obtained from Kaplan-Meier curve analyses. (B) Notch and NRF2 pathway proteins are differentially expressed in CC tissue samples. (C) Interactions among differentially expressed proteins in CC tissue samples. The colored lines represent the interaction source as follows: Experiments, pink; database, aqua blue; co-occurrence, navy blue; and co-expression, black. Created in STRING function network (version 12.0). An HR value of 1 means there is no difference between the groups. An HR value of 2 means there is double the risk of death. An HR value of 0.5 means that there is half the risk of patient death. Red indicates a higher risk level, while green means less risk. HR, hazard ratio; CIN, cervical intraepithelial neoplasia; PI3KCA; PIK3-catalytic subunit a; FAT1, FAT atypical cadherin; FBXW7, F-box and WD repeat domain containing 7; KEAP1, kelch-like ECH-associated protein 1; EP300, E1A-associated cellular p300 transcriptional co-activator protein; NRF2, nuclear factor erythroid 2-related factor 2; c-MYC, cellular-MYC; CREBBP, cAMP response element-binding binding protein; YAP1, yes-associated protein 1; TEAD2, TEA domain family member 2.

Protein level analysis through measurement of the percentage of positivity and intensity of protein expression levels of the tissue samples demonstrated that proteins from the NRF2 pathway were upregulated in all tumor samples compared with non-cancerous tissue samples. It has been well documented that the primary role of the NRF2 pathway is to detoxify cells by inducing the expression of antioxidant enzymes such as heme oxygenase, catalase, glutathione peroxidase and superoxide dismutase. These enzymes can neutralize ROS in the early stages of cancer development, which protects cells from damage by oxidative stress (25). However, the NRF2 pathway is also known for its dual action. In the tumor microenvironment, the NRF2/KEAP1 complex aids disease progression by the inactivation of chemotherapy drugs through ROS elimination, which protects cancer cells from drug-induced cell death (23,24). Based on the results of the present study, it could be suggested that this pair of genes are potential markers for the onset of cervical malignant neoplasia, as upregulation of NRF2 and inhibition of KEAP1 were observed even in the earliest stages of CC.

The NRF2/KEAP1 axis establishes crosstalk with the PI3K/AKT1 axis in cellular detoxification through ROS. Increased ROS levels activate this pathway through the inhibition of phosphatases, such as PTEN, or the activation of oncogenes, such as AKT (16,19). AKT1 biological functions

have been extensively studied and are linked to survival, proliferation, metabolism and cellular growth, all of which serve critical functions in carcinogenesis (34). In the present study, AKT1 protein expression levels were increased in the CIN 1 and CIN 2 stages of CC, suggesting that the early stages of CC may be supported by the AKT1 pathway. In addition, previous studies have demonstrated that the viral oncoproteins HPV E6 and E7 can induce activation of the AKT/PI3K pathway (35). PI3KCA serves a crucial role in cellular functions, such as growth, proliferation, differentiation, motility, survival and intracellular trafficking, and is often hyperactive in cancer, being attributed to certain roles in cancer development (36). In patients with CC, it was reported that an amplification of PI3KCA 3q26.3, the most common mutation of PI3KCA in CC, is implicated in the progression of cervical dysplastic cells towards invasive cancer (37). Consistently, the present study showed an increase in the PI3KCA expression levels in the *in situ* and invasive CC samples.

The expression levels of 12 proteins associated with the Hippo, Notch and NRF2 pathways that serve essential roles and are dysregulated in certain types of cancer, were analyzed in CC. The results demonstrated that in CC, the Hippo pathway did not show changes between tumor and normal samples. At the mRNA level, increased expression levels of c-MYC (Notch pathway) and AKT1 (NRF2 pathway),

and decreased levels of NRF2, showed an association with a reduced survival rate through Kaplan-Meier analysis. In the invasive stage of CC, high expression levels of c-MYC mRNA were demonstrated. NRF2 protein expression levels showed a significant change in all precancerous and cancerous stages samples compared with those in normal samples. The invasive stage samples also exhibited increased protein expression levels of PI3KCA, another protein from the NRF2/KEAP1 pathway family. CREBBP (Notch pathway) and PI3K (NRF2 pathway) were upregulated in the *in situ* CC samples. During earlier stages of CC, the AKT1 protein was upregulated. The present study indicates that the proteins of the Notch pathway (c-MYC and CREBBP) and the NRF2 pathway (NRF2/KEAP1 and AKT1) are essential and are dysregulated in CC.

Acknowledgements

Funding

Availability of data and materials

The data generated in the present study may be requested from the corresponding author.

Authors' contributions

GMA and VM were responsible for study conceptualization and experimental design. Experimental procedures and data analysis were performed by JELG, PAE, KIVS, RCO, FL, VM, JMZ, PPS and GMA. VM, JMZ and GMA prepared the manuscript draft. JELG, PAE, KIVS, RCO, FL and GMA were responsible for conceptualization and design of tables and figures. JELG, PAE, KIVS, RCO, FL, VM, JMZ, PPS and GMA participated in the writing, review and editing of the manuscript. JELG and GMA confirm the authenticity of all the raw data. GMA was responsible for funding acquisition. All authors have read and approved the final version of the manuscript.

Ethics approval and consent to participate

The study was conducted in accordance with the Declaration of Helsinki and approved by the Ethics Committee of Hospital General Zacatecas 'Luz Cosío González' (Mexico City, Mexico; approval no. 0131/2018; March 14, 2018) for the FFPE cervical tissue study. The FFPE tissues were obtained from hospital files ≥10 years of age. Therefore, according to the Hospital General Zacatecas policies, signed consent from patients was not necessary for the use of archived material.

Patient consent for publication

Not applicable.

Competing interests

The authors declare that they have no competing interests.

References

1. Singh D, Vignat J, Lorenzoni V, Eslahi M, Ginsburg O, Lauby-Secretan B, Arbyn M, Basu P, Bray F and Vaccarella S: Global estimates of incidence and mortality of cervical cancer in 2020: A baseline analysis of the WHO global cervical cancer elimination initiative. Lancet Glob Health 11: e197-e206, 2023.
2. Morales-Figueroa GG, Bravo-Parra M, Olivas-Matas KM, Esparza-Romero J, Valenzuela-Zamorano M, Olivas-López OM and Quihui-Cota L: Associated factors with human papillomavirus infection in adult women from northwest Mexico. Biotecnia 25: 133-139, 2022.
3. Ostroverkhova D, Przytycka TM and Panchenko AR: Cancer driver mutations: Predictions and reality. Trends Mol Med 29: 554-566, 2023.
4. Martínez-Jiménez F, Muiños F, Sentís I, Deu-Pons J, Reyes-Salazar I, Arnedo-Pac C, Mularoni L, Pich O, Bonet J, Kranas H, *et al*: A compendium of mutational cancer driver genes. Nat Rev Cancer 20: 555-572, 2020.
5. Uruno A and Yamamoto M: The KEAP1-NRF2 system and neurodegenerative diseases. Antioxid Redox Signal 38: 974-988, 2023.
6. Fox DB, Garcia NMG, McKinney BJ, Lupo R, Noteware LC, Newcomb R, Liu J, Locasale JW, Hirschey MD and Alvarez JV: NRF2 activation promotes the recurrence of dormant tumour cells through regulation of redox and nucleotide metabolism. Nat Metab 2: 318-334, 2020.
7. Guenter R, Patel Z and Chen H: Notch signaling in thyroid cancer. In: Notch Signaling in Embryology and Cancer. Vol. 1287 Reichrath J and Reichrath S (eds.) Springer International Publishing, Cham, pp155-168, 2021.
8. Llombart V and Mansour MR: Therapeutic targeting of 'undruggable' MYC. EBioMedicine 75: 103756, 2022.
9. Fu M, Hu Y, Lan T, Guan KL, Luo T and Luo M: The Hippo signalling pathway and its implications in human health and diseases. Signal Transduct Target Ther 7: 376, 2022.
10. Mendoza-Almanza G, Ortíz-Sánchez E, Rocha-Zavaleta L, Rivas-Santiago C, Esparza-Ibarra E and Olmos J: Cervical cancer stem cells and other leading factors associated with cervical cancer development. Oncol Lett 18: 3423-3432, 2019.
11. Sanchez-Vega F, Mina M, Armenia J, Chatila WK, Luna A, La KC, Dimitriadoy S, Liu DL, Kantheti HS, Saghafinia S, *et al*: Oncogenic signaling pathways in the cancer genome atlas. Cell 173: 321-337.e10, 2018.
12. Belder N, Coskun Ö, Doganay Erdogan B, Ilk O, Savas B, Ensari A and Özdağ H: From RNA isolation to microarray analysis: Comparison of methods in FFPE tissues. Pathol Res Pract 212: 678-685, 2016.
13. Farragher SM, Tanney A, Kennedy RD and Paul Harkin D: RNA expression analysis from formalin fixed paraffin embedded tissues. Histochem Cell Biol 130: 435-445, 2008.
14. Livak KJ and Schmittgen TD: Analysis of relative gene expression data using real-time quantitative PCR and the 2(-Delta Delta C(T)) method. Methods 25: 402-408, 2001.
15. Győrffy B: Discovery and ranking of the most robust prognostic biomarkers in serous ovarian cancer. Geroscience 45: 1889-1898, 2023.
16. Szklarczyk D, Franceschini A, Wyder S, Forslund K, Heller D, Huerta-Cepas J, Simonovic M, Roth A, Santos A, Tsafou KP *et al*: STRING v10: Protein-protein interaction networks, integrated over the tree of life. Nucleic Acids Res 43 (Database Issue): D447-D452, 2015.
17. Blokzijl A, Dahlqvist C, Reissmann E, Falk A, Moliner A, Lendahl U and Ibáñez CF: Cross-talk between the Notch and TGF-beta signaling pathways mediated by interaction of the Notch intracellular domain with Smad3. J Cell Biol 163: 723-728, 2003.
18. Papatheodorou I, Moreno P, Manning J, Muñoz-Pomer Fuentes A, George N, Fexova S, Fonseca NA, Füllgrabe A, Green M, Huang N, et al: Expression Atlas update: from tissues to single cells. Nucleic Acids Res 48: D77–D83, 2020.

19. Kma L and Baruah TJ: The interplay of ROS and the PI3K/Akt pathway in autophagy regulation. Biotechnol Appl Biochem 69: 248-264, 2022.
20. Mokhtari RB, Ashayeri N, Baghaie L, Sambi M, Satari K, Baluch N, Bosykh DA, Szewczuk MR and Chakraborty S: The Hippo pathway effectors YAP/TAZ-TEAD oncoproteins as emerging therapeutic targets in the tumor microenvironment. Cancers (Basel) 15: 3468, 2023.
21. Li X, Yan X, Wang Y, Kaur B, Han H and Yu J: The Notch signaling pathway: A potential target for cancer immunotherapy. J Hematol Oncol 16: 45, 2023.
22. Kar R, Jha SK, Ojha S, Sharma A, Dholpuria S, Raju VSR, Prasher P, Chellappan DK, Gupta G, Singh SK, *et al*: The FBXW7-NOTCH interactome: A ubiquitin proteasomal system-induced crosstalk modulating oncogenic transformation in human tissues. Cancer Rep (Hoboken) 4: e1369, 2021.
23. Panda H, Wen H, Suzuki M and Yamamoto M: Multifaceted roles of the KEAP1-NRF2 system in cancer and inflammatory disease milieu. Antioxidants (Basel) 11: 538, 2022.
24. Huang Y, Yang W, Yang L, Wang T, Li C, Yu J, Zhang P, Yin Y, Li R and Tao K: Nrf2 inhibition increases sensitivity to chemotherapy of colorectal cancer by promoting ferroptosis and pyroptosis. Sci Rep 13: 14359, 2023.
25. Aranda-Rivera AK, Cruz-Gregorio A, Arancibia-Hernández YL, Hernández-Cruz EY and Pedraza-Chaverri J: RONS and oxidative stress: An overview of basic concepts. Oxygen 2: 437-478, 2022.
26. Hanahan D: Hallmarks of cancer: New dimensions. Cancer Discov 12: 31-46, 2022.
27. Zhao Y, Shen M, Wu L, Yang H, Yao Y, Yang Q, Du J, Liu L, Li Y and Bai Y: Stromal cells in the tumor microenvironment: Accomplices of tumor progression? Cell Death Dis 14: 587, 2023.
28. Medda A, Compagnoni M, Spini G, Citro S, Croci O, Campaner S, Tagliabue M, Ansarin M and Chiocca S: c-MYC-dependent transcriptional inhibition of autophagy is implicated in cisplatin sensitivity in HPV-positive head and neck cancer. Cell Death Dis 14: 719, 2023.
29. Hareża DA, Wilczyński JR and Paradowska E: Human papillomaviruses as infectious agents in gynecological cancers. Oncogenic properties of viral proteins. Int J Mol Sci 23: 1818, 2022.
30. Peck B, Bland P, Mavrommati I, Muirhead G, Cottom H, Wai PT, Maguire SL, Barker HE, Morrison E, Kriplani D, *et al*: 3D functional genomics screens identify CREBBP as a targetable driver in aggressive triple-negative breast cancer. Cancer Res 81: 847-859, 2021.
31. Jiang Y, Guo X, Liu L, Rode S, Wang R, Liu H and Yang ZQ: Metagenomic characterization of lysine acetyltransferases in human cancer and their association with clinicopathologic features. Cancer Sci 111: 1829-1839, 2020.
32. Zhu Y, Wang Z, Li Y, Peng H, Liu J, Zhang J and Xiao X: The role of CREBBP/EP300 and its therapeutic implications in hematological malignancies. Cancers (Basel) 15: 1219, 2023.
33. Vannam R, Sayilgan J, Ojeda S, Karakyriakou B, Hu E, Kreuzer J, Morris R, Herrera Lopez XI, Rai S, Haas W, *et al*: Targeted degradation of the enhancer lysine acetyltransferases CBP and p300. Cell Chem Biol 28: 503-514.e12, 2021.
34. Hua H, Zhang H, Chen J, Wang J, Liu J and Jiang Y: Targeting Akt in cancer for precision therapy. J Hematol Oncol 14: 128, 2021.
35. Wang HM, Lu YJ, He L, Gu NJ, Wang SY, Qiu XS, Wang EH and Wu GP: HPV16 E6/E7 promote the translocation and glucose uptake of GLUT1 by PI3K/AKT pathway via relieving miR-451 inhibitory effect on CAB39 in lung cancer cells. Ther Adv Chronic Dis 11: 2040622320957143, 2020.
36. Tewari D, Patni P, Bishayee A, Sah AN and Bishayee A: Natural products targeting the PI3K-Akt-mTOR signaling pathway in cancer: A novel therapeutic strategy. Semin Cancer Biol 80: 1-17, 2022.
37. Voutsadakis IA: 3q26 amplifications in cervical squamous carcinomas. Curr Oncol 28: 2868-2880, 2021.